

# 3D-modeling from hip DXA shows improved bone structure with romosozumab followed by denosumab or alendronate

E. Michael Lewiecki<sup>1,\*</sup>, Donald Betah<sup>2</sup>, Ludovic Humbert<sup>3</sup>, Cesar Libanati<sup>4</sup>, Mary Oates<sup>2</sup>, Yifei Shi<sup>2</sup>, Renaud Winzenrieth<sup>3</sup>, Serge Ferrari<sup>5</sup>, Fumitoshi Omura<sup>6</sup>

- <sup>1</sup>New Mexico Clinical Research & Osteoporosis Center, 300 Oak St NE, Albuquerque, NM 87106, United States
- <sup>2</sup>Amgen Inc., One Amgen Center Drive, Thousand Oaks, CA 91320, United States
- <sup>3</sup>3D-SHAPER Medical, Rambla de Catalunya, 53, 4-H, Eixample, 08007 Barcelona, Spain
- <sup>4</sup>UCB Pharma, Allée de la Recherche, 60, Brussels B-1070, Belgium
- <sup>5</sup>Division of Bone Diseases, University Hospital of Geneva, Geneva 1211, Switzerland
- <sup>6</sup>Koenji Orthopedics Clinic, 4-29-2, Koenji minami, Suqinami-ku, Tokyo, 166-0003, Japan
- \*Corresponding author. E. Michael Lewiecki, New Mexico Clinical Research & Osteoporosis Center, 300 Oak St. NE, Albuquerque, NM 87106, United States. (mlewiecki@gmail.com).

### **Abstract**

Romosozumab treatment in women with postmenopausal osteoporosis increases bone formation while decreasing bone resorption, resulting in large BMD gains to reduce fracture risk within 1 yr. DXA-based 3D modeling of the hip was used to assess estimated changes in cortical and trabecular bone parameters and map the distribution of 3D changes in bone parameters over time in patients from 2 randomized controlled clinical trials: FRAME (romosozumab vs placebo followed by denosumab) and ARCH (romosozumab vs alendronate followed by alendronate). For each study, data from a subset of  $\sim$ 200 women per treatment group who had TH DXA scans at baseline and months 12 and 24 and had provided consent for future research were analyzed post hoc. 3D-SHAPER software v2.11 (3D-SHAPER Medical) was used to generate patient-specific 3D models from TH DXA scans. Percentage changes from baseline to months 12 and 24 in areal BMD (aBMD), integral volumetric BMD (vBMD), cortical thickness, cortical vBMD, cortical surface BMD (sBMD), and trabecular vBMD were evaluated. Data from 377 women from FRAME (placebo, 190; romosozumab, 187) and 368 women from ARCH (alendronate, 185; romosozumab, 183) with evaluable 3D assessments at baseline and months 12 and 24 were analyzed. At month 12, treatment with romosozumab vs placebo in FRAME and romosozumab vs alendronate in ARCH resulted in greater increases in aBMD, integral vBMD, cortical thickness, cortical vBMD, cortical sBMD, and trabecular vBMD (P < .05 for all). At month 24, cumulative gains in all parameters were greater in the romosozumab-to-denosumab vs placebo-to-denosumab sequence and romosozumab-to-alendronate vs alendronate-to-alendronate sequence (P < .05 for all). 3D-SHAPER analysis provides a novel technique for estimating changes in cortical and trabecular parameters from standard hip DXA images. These data add to the accumulating evidence that romosozumab improves hip bone density and structure, thereby contributing to the antifracture efficacy of the drug.

Keywords: cortical thickness, cortical volumetric BMD, cortical surface BMD, osteoporosis, trabecular volumetric BMD

### Lay Summary

Osteoporosis is a chronic condition in which bones become weak and are more likely to break (fracture) with minimal force such as tripping or falling. A fracture, especially in the elderly, is a serious condition that affects daily activities and quality of life. Romosozumab, an approved medication for patients with osteoporosis, increases bone mass and bone strength thereby reducing fracture risk. In this study, 3D reproductions of patients' hip bones were generated from standard images of a bone density test with DXA from women in the FRAME clinical trial where they received romosozumab or placebo for 12 mo followed by 12 mo of denosumab or the ARCH clinical trial where they received romosozumab or alendronate for 12 mo, followed by 12 mo of alendronate. We found that patients treated with romosozumab for the first 12 mo had significantly greater increases in bone strength compared with those who received placebo or alendronate. After 24 mo, total gains in bone strength measurements were greater in patients treated with romosozumab first. Our study shows that DXA-based 3D modelling provides a novel technique for examining changes in bone strength and supports the use of romosozumab to improve hip bone strength and reduce fracture risk.

### Introduction

Osteoporotic fractures are a consequence of deteriorated bone strength resulting from loss of bone mass and compromised bone microstructure, with hip fractures associated with high mortality and morbidity. The efficacy of any

therapeutic agent for osteoporosis treatment depends on its ability to increase bone strength and reduce fracture risk,<sup>6-13</sup> especially at the hip and spine.<sup>13</sup> However, direct measurement of bone strength in human subjects is not feasible.<sup>14</sup> Areal bone mineral density (aBMD), measured by

2-dimensional (2D) DXA, is the most commonly used method for assessing treatment effects of osteoporosis therapeutic agents. Although aBMD correlates with bone strength, is does not inform on all factors that determine bone strength, such as changes in macrostructure and microarchitecture, and also does not distinguish between effects on cortical and trabecular bone compartments, which may be differentially affected by different therapeutic agents. 2,16-19

QCT is an alternative approach used to assess bone strength. 14,20 This technique can differentiate between the effects of osteoporosis treatments on cortical vs trabecular bone compartments. However, QCT is not widely available in clinical practice and involves greater exposure to ionizing radiation than DXA. DXA-based 3-dimensional (3D) modeling can potentially overcome the limitations of QCT. DXA-based 3D modeling uses a statistical 3D shape and density model of the proximal femur built from a database of QCT scans to generate a patient-specific 3D model using a standard hip DXA scan<sup>21</sup>,<sup>22</sup> (Figure 1). DXA-based 3D modeling also provides a way to map the distribution of bone changes in cortical vs trabecular bone compartments for studies with no QCT measurements and to generate outputs for clinicians to visualize and monitor the effects of osteoporosis treatment.<sup>23-25</sup> Additionally, DXA-based 3D modeling has been used to demonstrate the differential effects of abaloparatide and teriparatide on hip cortical volumetric bone mineral density (vBMD) and of abaloparatide on bone strength, 23,24 and the effects of sequential therapy with abaloparatide followed by alendronate on the proximal femur in postmenopausal women with osteoporosis.<sup>23</sup>

DXA-based 3D modeling has been validated, with high correlation coefficients (R) reported between DXA-based 3D modeling and QCT-based measurements for vBMD of the cortical bone (R = 0.93) and trabecular bone (R = 0.86).<sup>21</sup> In addition, in a case–control study, DXA-derived 3D modeling measurements were found to be associated with incidence of hip fracture.<sup>26</sup>

Romosozumab is a bone-forming agent with the dual effect of increasing bone formation and decreasing bone resorption, 27,28 and is approved in multiple countries for the treatment of osteoporosis. Monthly subcutaneous romosozumab 210 mg for 12 mo produced larger gains in LS and TH aBMD by DXA<sup>27,29</sup> and reduced the risk of fractures compared with placebo in the Fracture Study in Postmenopausal Women With Osteoporosis (FRAME)<sup>30</sup> or compared with alendronate in the Active-Controlled Fracture Study in Postmenopausal Women With Osteoporosis at High Risk (ARCH).<sup>31</sup> These improvements were maintained when romosozumab was followed by an antiresorptive; that is, denosumab (a fully human monoclonal antibody against RANKL) in FRAME<sup>30</sup> or alendronate (a bisphosphonate) in ARCH.<sup>31</sup> QCT analysis in ARCH showed that romosozumab treatment resulted in greater gains in cortical and trabecular vBMD, BMC, and bone strength at the LS at months 6 and 12 compared with alendronate, with the most newly formed bone accruing in the cortical compartment.<sup>32</sup>

Here, we report results from a post hoc analysis using DXA-based 3D modeling of the hip to assess estimated changes in cortical and trabecular bone parameters and to map the distribution of 3D changes in the bone parameters over time in patients from FRAME (romosozumab vs placebo followed by denosumab)<sup>30</sup> and ARCH (romosozumab vs alendronate followed by alendronate).<sup>31</sup>

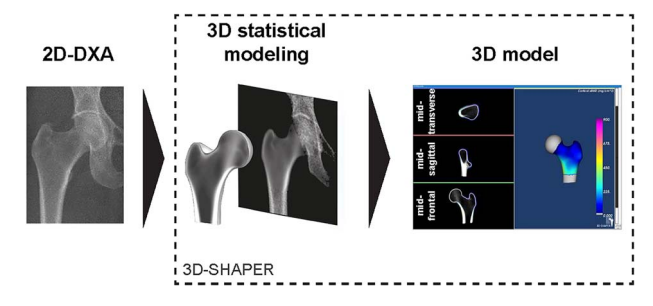


**Figure 1.** 3D model creation using standard hip DXA scans. DXA-based 3D modeling uses a statistical 3D shape and density model of the proximal femur built from a database of QCT scans to generate a patient-specific 3D model using a standard hip DXA scan. The color scale indicates the anatomical distribution of the cortical surface BMD, expressed in mg/cm<sup>2</sup>.

### Patients and methods Study designs and patients

The study designs for FRAME<sup>30</sup> (NCT01575834) and ARCH<sup>31</sup> (NCT01631214) randomized controlled trials are illustrated in Supplementary Figure S1. For each of the 2 trials, data from a subset of  $\sim$ 200 selected women per treatment group who had completed the 24-mo study period, had provided consent for future research, and had TH DXA scans at baseline and at months 12 and 24 were included in the current post hoc analysis.

FRAME<sup>30</sup> had randomized 7180 postmenopausal women aged 55 to 90 yr, with a T-score of -2.5 to -3.5 at the TH or FN, and no history of hip fracture or any severe or > 2 moderate vertebral fractures. The women received double-blinded monthly subcutaneous romosozumab 210 mg or placebo for 12 mo, after which both groups received open-label subcutaneous denosumab 60 mg every 6 mo for an additional 12 mo (Supplementary Figure \$1A). The co-primary endpoints were the cumulative incidences of new vertebral fractures at months 12 and 24; key secondary endpoints included incidences of clinical and nonvertebral fractures and changes in aBMD at months 12 and 24.30 aBMD was assessed by DXA, and vertebral fracture incidence was assessed by spinal radiographs at baseline and at months 12 and 24. Results for the primary and secondary endpoints have been previously published.<sup>30</sup> In the current analysis, DXA-based 3D modeling was performed on data from a subset of ~200 women per treatment group who had completed the 24-mo study period, had provided consent for future research, and had TH DXA scans at baseline, month 12, and month 24. This population included data from 122 women (61 in each treatment group) enrolled in the protocol-prespecified FRAME DXA substudy and 140 randomly selected women per treatment group from FRAME who were not enrolled in the FRAME DXA substudy. Since the protocol-prespecified FRAME DXA substudy included postbaseline TH DXA scans at month 6, in addition to DXA scans at months 12 and 24, the current analysis using DXAbased 3D modeling was also performed separately for the FRAME DXA substudy population who had completed the 24-mo study period, had provided consent for future research, and had TH DXA scans at baseline, month 6, month 12, and month 24. aBMD by DXA was also determined for the subset of ~200 women in each treatment group included in the current analysis.

ARCH<sup>31</sup> had randomized 4093 postmenopausal women with osteoporosis aged 55 to 90 yr with one of the following: T-score  $\leq$  -2.5 at the TH or FN and either  $\geq$ 1 moderate or severe vertebral fracture or > 2 mild vertebral fractures; or Tscore < -2.0 at the TH or FN and either > 2 moderate or severe vertebral fractures or a fracture of the proximal femur sustained 3 to 24 mo before randomization. The women received double-blinded monthly subcutaneous romosozumab 210 mg or weekly oral alendronate 70 mg for 12 mo, followed by open-label weekly oral alendronate 70 mg in both groups (Supplementary Figure S1B). The primary endpoints were the cumulative incidence of new vertebral fracture at 24 mo and the cumulative incidence of clinical fracture at the time of the primary analysis (performed after clinical fractures had been confirmed in >330 patients and all the patients had completed the month 24 visit).<sup>31</sup> Key secondary endpoints included the incidence of nonvertebral fracture at the time of the primary analysis and through months 12 and 24, and changes in aBMD at months 12 and 24. aBMD and vertebral fracture incidence were evaluated by DXA and spinal radiographs, respectively, at baseline and at months 12 and 24. Results for the primary and secondary endpoints have been previously published.<sup>31</sup> In the current analysis, DXA-based 3D modeling was performed on data from a subset of ~200 randomly selected women per treatment group who had completed the 24-mo study period, had provided consent for future research, and had TH DXA scans at baseline, month 12, and month 24. aBMD by DXA was also determined for the subset of ~200 women in each treatment group included in the current analysis.

### **DXA-based 3D modeling**

Image files of hip DXA scans taken at baseline, month 12, and month 24 in FRAME and ARCH were analyzed by DXA-based 3D modeling using 3D-SHAPER software v2.11 (3D-SHAPER Medical, Barcelona, Spain) as previously described, 21,22 with operators blinded to treatment. Briefly, the 3D-SHAPER software uses a statistical model based on a database of QCT scans from Caucasian men and women to generate a 3D patient-specific model of the proximal femur that allows for a separate characterization of the cortical and trabecular bone compartments<sup>21,22</sup> (Figure 1). Integral vBMD (expressed in mg/cm<sup>3</sup>) was calculated as the mean vBMD of the integral (ie, cortical and trabecular) compartment at the TH region. The cortical bone was segmented by fitting a function of cortical thickness (expressed in mm), cortical vBMD (expressed in mg/cm<sup>3</sup>), location of the cortex, density of surrounding tissues, and imaging blur to the density profile computed along the normal vector at each node of the proximal femur surface mesh.<sup>22</sup> Cortical surface BMD (sBMD; a measure of the density-to-thickness ratio expressed in mg/cm<sup>2</sup>) was calculated as the product of cortical vBMD and cortical thickness at each vertex of the femoral surface of the 3D model.<sup>21,22</sup> As cortical sBMD measures both the cortical thickness and density, it can be used as a surrogate parameter for cortical bone strength.<sup>24</sup> Mean cortical thickness, mean cortical vBMD, and mean cortical sBMD were computed at the TH region. Trabecular vBMD (expressed in mg/cm<sup>3</sup>) was calculated using the output 3D image as the average vBMD of the trabecular compartments at the TH region.

### Anatomical distribution of changes in bone structure

The 3D data generated from the hip DXA scans in FRAME and ARCH were used to calculate average 3D models and assess the anatomical distribution of changes in bone structure in each treatment group. One average, 3D model per time point (baseline, month 12, and month 24) and treatment group was generated using image registration techniques. For each treatment group, the average 3D models obtained at month 12 and month 24 were compared with baseline to assess the anatomical distribution of the changes in bone structure. Changes in cortical thickness, cortical vBMD, and cortical sBMD were displayed at the periosteal surface of the femur using 3D visualizations; changes in cortical and trabecular vBMD were displayed using cross-sectional images.<sup>23</sup>

### Statistical analysis

In FRAME, treatment group comparisons for percentage change from baseline to months 12 and 24 for aBMD, integral vBMD, cortical thickness, cortical vBMD, cortical sBMD, and trabecular vBMD were assessed by a repeatedmeasures model adjusting for treatment, visit, treatment-byvisit interaction, baseline value, machine type, and baseline value-by-machine type interaction. Similarly, in the FRAME DXA substudy population, treatment group comparisons for percentage change from baseline to months 6, 12, and 24 were evaluated by a repeated-measures model adjusting for these same factors. In ARCH, treatment group comparisons for percentage change from baseline to months 12 and 24 for aBMD, integral BMD, cortical thickness, cortical vBMD, cortical sBMD, and trabecular vBMD were assessed by a repeated-measures model adjusting for treatment, presence of severe vertebral fracture at baseline, visit, treatment-by-visit interaction, baseline value, machine type, and baseline valueby-machine type interaction. Percentage change from baseline was reported as least squares (LS) means and associated 95% CI. No adjustments for multiplicity were made, and there was no imputation of missing data.

### **Results**

### Patients and baseline characteristics

In FRAME, 402 women were selected for the DXA-based 3D-SHAPER analysis. Of these, 377 had evaluable 3D assessments at baseline, month 12, and month 24 (placebo, 190; romosozumab, 187) and were included in the analysis (Figure 2). This included 104 women who had enrolled in the prespecified FRAME DXA substudy (placebo, 56; romosozumab, 48). A total of 25 women were excluded from the analysis (placebo, 11; romosozumab, 14) because the DXA scanner or the DXA acquisition mode used for 3D assessment was not supported by the 3D-SHAPER software or because of missing follow-up data points. In ARCH, 400 women were selected for the DXA-based 3D-SHAPER analysis. Of these, 368 had evaluable 3D assessments at baseline, month 12, and month 24 (alendronate, 185; romosozumab, 183) (Figure 3) and were included in the analysis. A total of 32 women were excluded from the analysis (alendronate, 15; romosozumab, 17) because the DXA scanner or the DXA acquisition mode used for 3D assessment was not supported

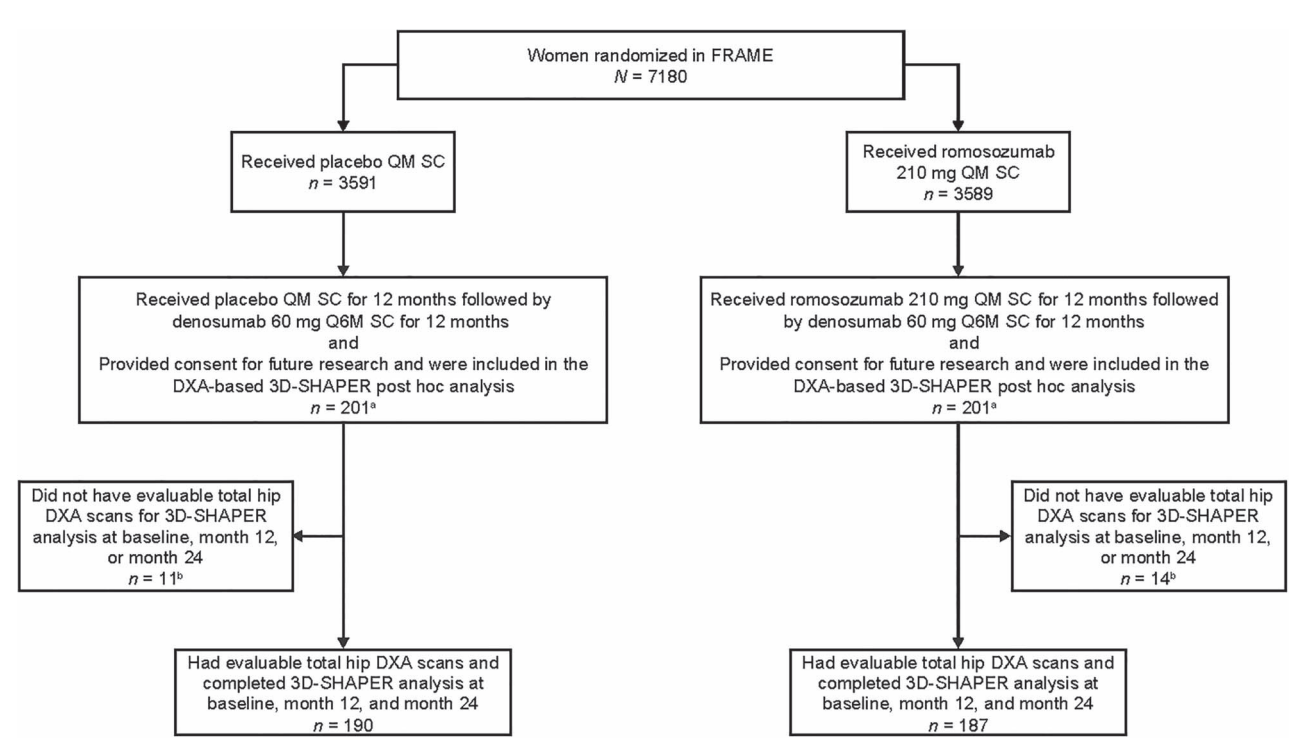


**Figure 2.** Patient disposition of the select subpopulation evaluated in the DXA-based 3D-SHAPER post hoc analysis in FRAME. <sup>a</sup>The FRAME population for the DXA-based 3D-SHAPER post hoc analysis included a total of 402 women (201 per treatment group); the 402 women included 122 women (61 placebo, 61 romosozumab) enrolled in the prespecified FRAME DXA substudy and 280 randomly selected women (140 placebo, 140 romosozumab) from FRAME who were not enrolled in the FRAME DXA substudy. <sup>b</sup>Women were excluded because the DXA scanner or the DXA acquisition mode used for 3D assessment was not supported by 3D-SHAPER software or because of missing follow-up data points.

by the 3D-SHAPER software or because of missing follow-up data points.

Baseline characteristics for the women in the post hoc DXAbased 3D-SHAPER analysis were consistent with the recruitment criteria for each study and consistent with the baseline characteristics for the overall populations for each study (Table 1, Supplementary Table S1, Supplementary Table S2). In FRAME, which had enrolled women with less severe osteoporosis, the mean (SD) age was 70.3 (7.4) yr and mean (SD) baseline T-scores were -2.8 (1.0) at the LS, -2.4 (0.5) at the TH, and -2.7 (0.3) at the FN for the FRAME 3D-SHAPER analysis population (Table 1, Supplementary Table S1). Less than 20% of the women had a vertebral fracture (19.1%) and a nonvertebral fracture (19.4%) at baseline. Similar baseline characteristics were observed for the FRAME DXA substudy 3D-SHAPER analysis population (Supplementary Table S1). In ARCH, which enrolled older women with low BMD and at least one prevalent fracture, mean (SD) age was 73.4 (7.1) yr and mean (SD) baseline T-scores were -3.0 (1.2) at the LS, -2.8 (0.6) at the TH, and -2.9 (0.4) at the FN for the ARCH 3D-SHAPER analysis population (Table 1, Supplementary Table S2). In the ARCH 3D-SHAPER analysis population, 95.9% of women had a vertebral fracture and 37.5% had a nonvertebral fracture at baseline.

## Percentage changes from baseline in hip aBMD by 2D-DXA and estimated integral vBMD by DXA-based 3D-SHAPER analysis

Integral bone density was measured as aBMD determined by 2D-DXA and as integral vBMD determined by 3D-SHAPER analysis. In FRAME, treatment with romosozumab vs placebo for 12 mo resulted in significantly greater increases in aBMD

by 2D-DXA and similarly resulted in significantly greater increases in estimated integral vBMD by DXA-based 3D-SHAPER analysis, with LS mean percentage change from baseline of 6.6% vs 0.4% for aBMD (Figure 4A) and 7.4% vs 0.3% for integral vBMD (Figure 4C) (P < .001 for both bone parameters). At month 24, the cumulative gains were significantly greater in the romosozumab-to-denosumab sequence vs the placebo-to-denosumab sequence by both 2D-DXA and DXA-based 3D-SHAPER analysis, with LS mean percentage change from baseline of 8.7% vs 3.3% for aBMD and 9.3% vs 3.6% for integral vBMD (P < .001 for both bone parameters). Also in ARCH, treatment with romosozumab vs alendronate for 12 mo resulted in significantly greater increases in aBMD by 2D-DXA and similarly resulted in significantly greater increases in estimated integral vBMD by 3D-SHAPER analysis, with LS mean percentage change from baseline of 6.6% vs 2.8% for aBMD (Figure 4B) and 7.1% vs 2.7% for integral vBMD (Figure 4D) (P < .001 for both bone parameters). At month 24, the cumulative gains were significantly greater in the romosozumab-to-alendronate sequence vs the alendronate-to-alendronate sequence by both 2D-DXA and DXA-based 3D-SHAPER analysis, with LS mean percentage change from baseline of 7.4% vs 3.7% for aBMD and 7.7% vs 3.4% for integral vBMD (P < .001 for both bone parameters).

# Percentage changes from baseline in estimated hip cortical thickness, cortical vBMD, cortical sBMD, and trabecular vBMD by DXA-based 3D-SHAPER analysis

Computed percentage changes from baseline to month 12 and month 24 in hip cortical thickness, cortical vBMD, cortical sBMD, and trabecular vBMD are topographically shown in

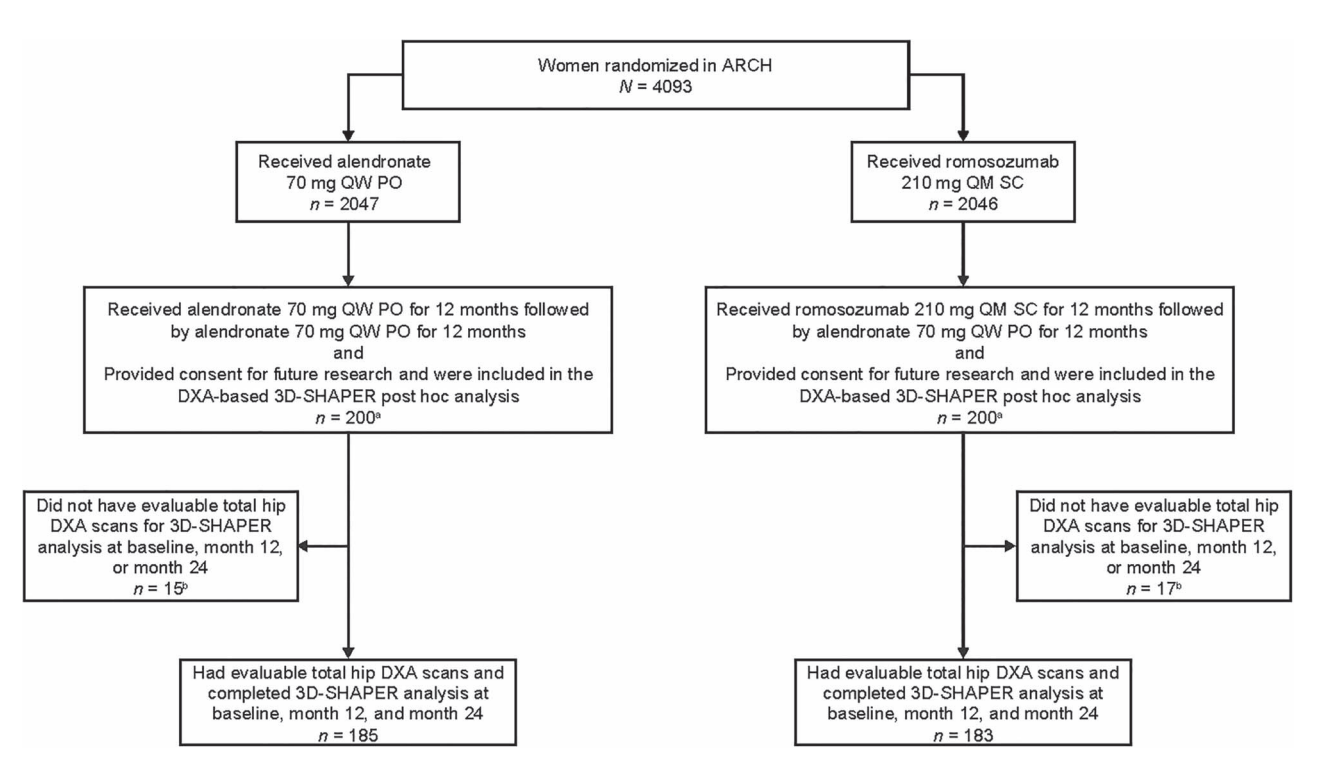


**Figure 3.** Patient disposition of the select subpopulation evaluated in the DXA-based 3D-SHAPER post hoc analysis in ARCH. <sup>a</sup>The ARCH population for the DXA-based 3D-SHAPER post hoc analysis included a total of 400 randomly selected women (200 per treatment group). <sup>b</sup>Women were excluded because the DXA scanner or the DXA acquisition mode used for 3D assessment was not supported by the 3D-SHAPER software or because of missing follow-up data points.

Table 1. Baseline characteristics of women included in the FRAME 3D-SHAPER analysis population and the ARCH 3D-SHAPER analysis population.

Characteristic	FRAME 3D-SHAPER analysis population		ARCH 3D-SHAPER analysis population	
	Placebo-to- denosumab n = 190	Romosozumab-to- denosumab n = 187	Alendronate-to- alendronate n = 185	Romosozumab-to- alendronate n = 183
$\overline{\text{Age, yr, mean} \pm \text{SD}}$	$70.2 \pm 7.4$	$70.3 \pm 7.5$	$72.9 \pm 7.3$	$73.8 \pm 7.0$
BMD T-score, mean $\pm$ SD				
LS	$-2.8 \pm 1.0$	$-2.8 \pm 1.0$	$-3.0 \pm 1.1$	$-3.0 \pm 1.3$
TH	$-2.4 \pm 0.5$	$-2.4 \pm 0.5$	$-2.7 \pm 0.6$	$-2.8 \pm 0.6$
FN	$-2.7 \pm 0.3$	$-2.8 \pm 0.3$	$-2.9 \pm 0.4$	$-2.9 \pm 0.4$
Prevalent vertebral fracture, <i>n</i> (%)	42 (22.1)	30 (16.0)	177 (95.7)	176 (96.2)
Previous nonvertebral fracture at $\geq$ 45 yr of age, $n$ (%)	35 (18.4)	38 (20.3)	63 (34.1)	75 (41.0)
FRAX MOF calculated with BMD, mean % ± SD	$10.9 \pm 6.7$	$12.3 \pm 8.0$	$19.3 \pm 9.4$	$19.5 \pm 9.5$
FRAX hip fracture calculated with BMD, mean $\% \pm SD$	$4.7 \pm 4.3$	$5.3 \pm 4.9$	$9.4 \pm 6.9$	$9.6 \pm 7.2$

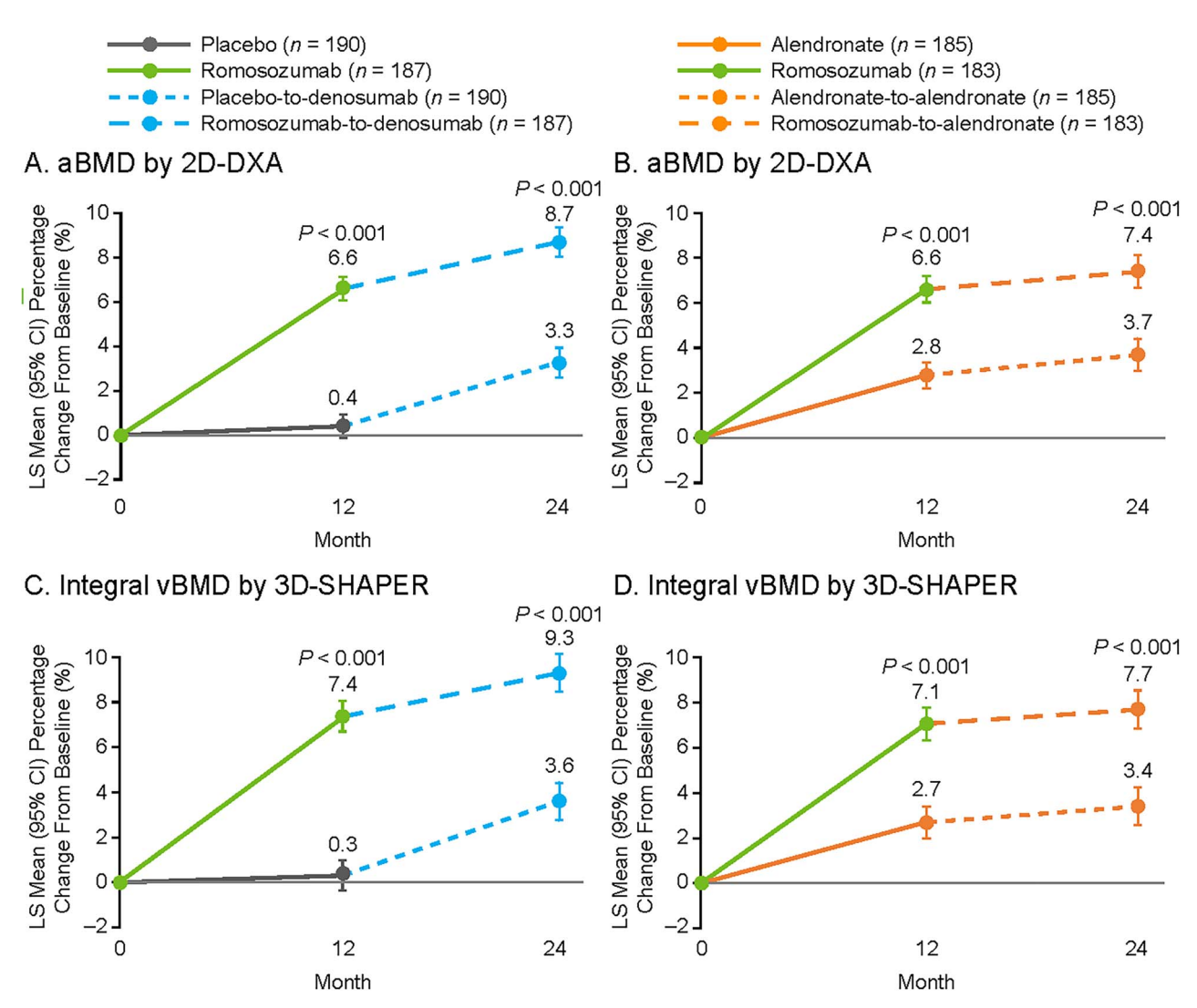
*n* = no. of women who had completed the 24-mo study period, had provided consent for future research, had TH DXA scans at baseline, month 12, and month 24, and completed the 3D-SHAPER analysis. Abbreviations: 3D, 3-dimensional; ARCH, Active-Controlled Fracture study in Postmenopausal Women with Osteoporosis at High Risk; FRAME, Fracture Study in Postmenopausal Women with Osteoporosis; FRAX, 10-yr probability of fracture; MOF, major osteoporotic fracture.

Figure 5 for FRAME and Figure 6 for ARCH and illustrated in animated videos in Supplementary Figure S2 (Supplementary Video S1) for both studies. The percentage changes from baseline to month 12 and month 24 in these parameters are then shown graphed in Figure 7.

In FRAME, treatment with romosozumab vs placebo for 12 mo resulted in significantly greater increases in estimated bone parameters (Figure 5, Figure 7, Supplementary Figure S2 [Supplementary Video S1]), with LS mean percentage change from baseline of 2.9% vs 0.2% for cortical thickness (Figure 7A), 2.8% vs 0% for cortical vBMD (Figure 7C), 5.8% vs 0.2% for cortical sBMD (Figure 7E), and 12.4% vs 1.3% for trabecular vBMD (Figure 7G) (P < .001 for all bone parameters). At month 24, the cumulative gains

were significantly greater in the romosozumab-to-denosumab sequence vs the placebo-to-denosumab sequence, with LS mean percentage change from baseline of 4.0% vs 1.2% for cortical thickness, 4.2% vs 1.8% for cortical vBMD, 8.6% vs 3.0% for cortical sBMD, and 13.7% vs 5.2% for trabecular vBMD (P < .001 for all bone parameters). Results for the 104 women in the FRAME DXA substudy showed that significantly greater increases in estimated bone parameters were seen as early as 6 mo after romosozumab treatment, with results at months 12 and 24 similar to those of the 377 women in the FRAME 3D-SHAPER analysis population described above (Supplementary Figure S3).

In ARCH, treatment with romosozumab vs alendronate for 12 mo resulted in significantly greater increases in estimated



**Figure 4.** Percentage change from baseline to month 12 and month 24 in aBMD by 2D-DXA and integral vBMD by 3D-SHAPER analysis of hip DXA scans in FRAME (A and C) and ARCH (B and D). n = no. of women who had completed the 24-mo study period, had provided consent for future research, had TH DXA scans at baseline, month 12, and month 24, and completed the 3D-SHAPER analysis. Treatment group comparisons for percentage change from baseline for aBMD by 2D-DXA and integral vBMD by DXA-based 3D-SHAPER analysis were assessed by a repeated-measures model adjusting for treatment, visit, treatment-by-visit interaction, baseline value, machine type and baseline value-by-machine type interaction in FRAME and adjusting for treatment, presence of severe vertebral fracture at baseline, visit, treatment-by-visit interaction, baseline value, machine type and baseline value-by-machine type interaction in ARCH. P values are for the comparison of the 2 treatment groups in each study.

bone parameters (Figure 6, Figure 7, Supplementary Figure S2, [Supplementary Video S1]), with LS mean percentage change from baseline of 2.1% vs 1.2% (P = .010) for cortical thickness (Figure 7B), 2.6% vs 1.7% (P = .013) for cortical vBMD (Figure 7D), 4.7% vs 2.9% (P < .001) for cortical sBMD (Figure 7F), and 13.6% vs 3.3% (P < .001) for trabecular vBMD (Figure 7H). At month 24, the cumulative gains were significantly greater in the romosozumab-to-alendronate sequence vs the alendronate-to-alendronate sequence, with LS mean percentage change from baseline of 2.7% vs 1.1% (P < .001) for cortical thickness, 3.3% vs 2.5% (P = .035) for cortical vBMD, 6.1% vs 3.5% (P < .001) for cortical sBMD, and 13.0% vs 4.6% (P < .001) for trabecular vBMD.

### **Discussion**

In this study, we applied DXA-based 3D modeling by 3D-SHAPER analysis of standard hip DXA scans to assess

hip cortical and trabecular bone changes in patients from the FRAME and ARCH clinical trials. At month 12, treatment with romosozumab resulted in significantly greater increases in aBMD, integral vBMD, cortical thickness, cortical vBMD, cortical sBMD, and trabecular vBMD compared with placebo in FRAME, and compared with alendronate in ARCH. At month 24, the cumulative gains in these bone parameters were significantly greater in the romosozumab-to-denosumab vs placebo-to-denosumab sequence in FRAME and romosozumab-to-alendronate vs alendronate-to-alendronate sequence in ARCH.

Results from our analysis add to the growing evidence that the observed efficacy of romosozumab in reducing fracture risk compared with placebo in FRAME<sup>30</sup> or alendronate in ARCH<sup>31</sup> is associated with improvements in bone parameters.<sup>11,32-36</sup> As expected, the significantly greater increases in hip aBMD with romosozumab treatment compared with placebo treatment in FRAME and alendronate

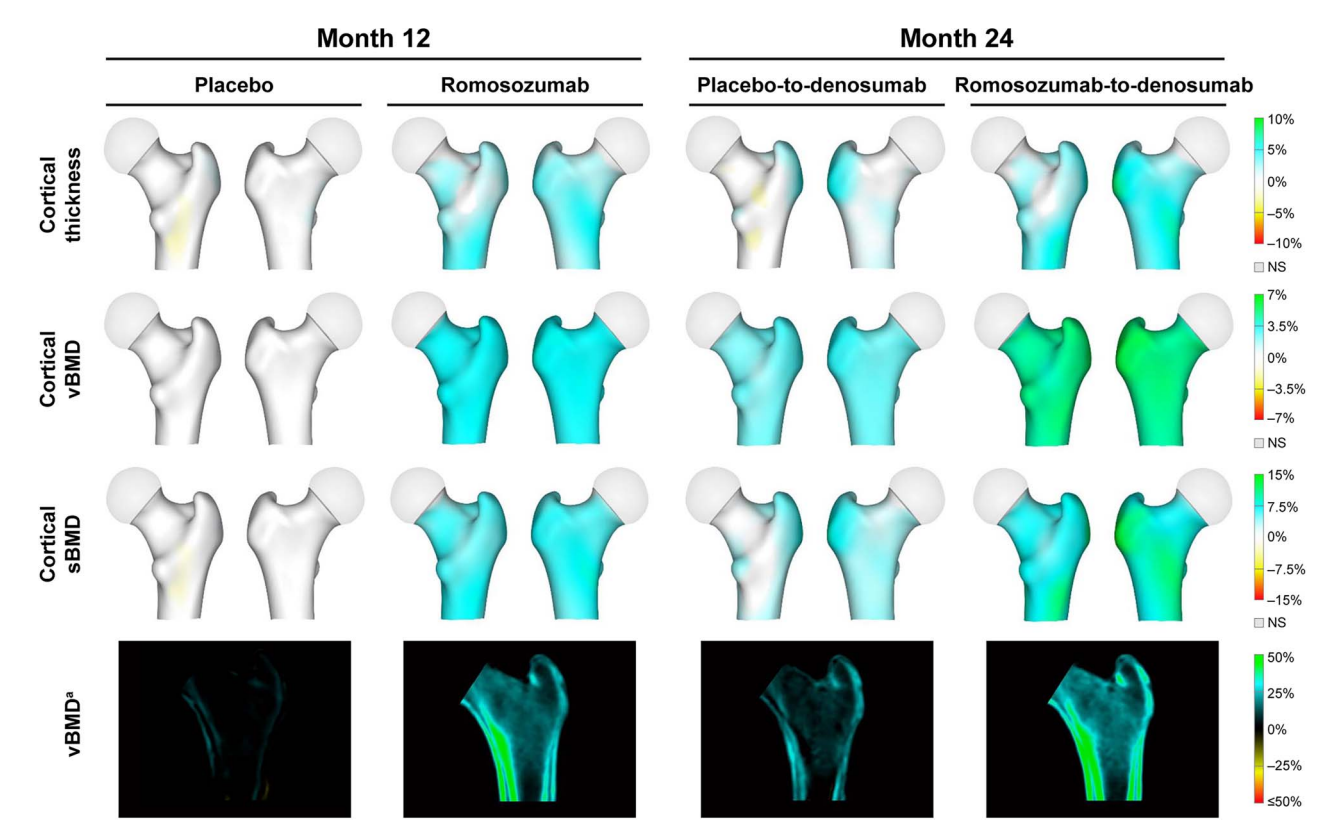


**Figure 5.** Percentage change from baseline to month 12 and month 24 in cortical thickness, cortical vBMD, cortical sBMD, and vBMD for cortical and trabecular compartments by 3D-SHAPER analysis of hip DXA scans in FRAME. Increases in bone parameters are presented in blue–green color; decreases are presented in yellow–red color. Illustrations for each pair of representative femurs per treatment group show the posterior anterior perspective on the left and the anterior posterior perspective on the right. <sup>a</sup>vBMD images include cortical and trabecular compartments; images and data are from a mid-coronal slice. NS, not significant against baseline, Student"s *t*-test;

treatment in ARCH in the subpopulations included in the current analysis as determined by 2D-DXA were consistent with previously reported increases in hip aBMD in the overall FRAME and ARCH populations as also determined by 2D-DXA.<sup>30,31</sup> Observed changes in integral bone density were similar when measured as aBMD determined by 2D-DXA and when measured as integral vBMD determined by 3D-SHAPER analysis, with significantly greater increases in aBMD and integral vBMD after romosozumab vs placebo treatment in FRAME and after romosozumab vs alendronate treatment in ARCH. In a QCT analysis of data from a subset of treatment-naïve patients with low BMD in a romosozumab phase 2 dose-ranging study, 12 mo of treatment with romosozumab significantly increased hip integral and trabecular vBMD vs 12 mo of treatment with placebo or teriparatide<sup>34</sup> and was associated with bone-strengthening effects as estimated by finite element analysis.<sup>36</sup> Although the no. of patients analyzed by QCT in the phase 2 study was small (romosozumab, n = 9; placebo, n = 18; teriparatide, n = 19)<sup>34</sup> and the results should be interpreted with caution, the QCT findings are consistent with findings from the current analysis that treatment with romosozumab vs placebo in FRAME or vs alendronate in ARCH significantly increased hip integral and trabecular vBMD as measured by DXA-based 3D-SHAPER analysis. However, although findings from the phase 2 study showed similar changes in hip cortical vBMD with romosozumab, placebo, and teriparatide, the current analysis showed a significantly greater increase in hip cortical vBMD with romosozumab vs placebo or alendronate. It is

unclear why data obtained by QCT and DXA-based 3D-SHAPER for romosozumab treatment on hip integral and trabecular vBMD were similar across the studies but differed for cortical vBMD. As hip QCT data are not available for the FRAME and ARCH studies, a direct comparison of QCT data with the 3D-SHAPER data reported here was not possible.

The strength of our analysis is that it used data from 2 randomized controlled studies with standard assessments of BMD and bone parameters, and documented fracture risk reductions. However, there are limitations to consider. First, only 377 of 7180 women in FRAME (~5%) and 368 of 4093 women in ARCH (~9%) were included in the DXA-based 3D-SHAPER analysis; thus, it is possible that the subpopulations analyzed are not representative of the total populations of the studies. Second, although other studies have evaluated the effect of romosozumab treatment on changes in bone parameters by QCT, we cannot compare data from the FRAME and ARCH DXA-based 3D-SHAPER analysis with data from other studies derived by QCT because of differences in skeletal sites evaluated in the studies and/or differences in study populations. 11,32-35

Differences between results generated using DXA-based 3D-SHAPER and those generated using QCT have been observed. As reported in previous studies, <sup>21,37</sup> spatial resolution of 3D-SHAPER models is lower than that of QCT, which might result in larger errors when measuring cortical or trabecular parameters locally in small regions of interest. In particular, larger errors reported at the lesser trochanter region should be considered when assessing bone changes in this

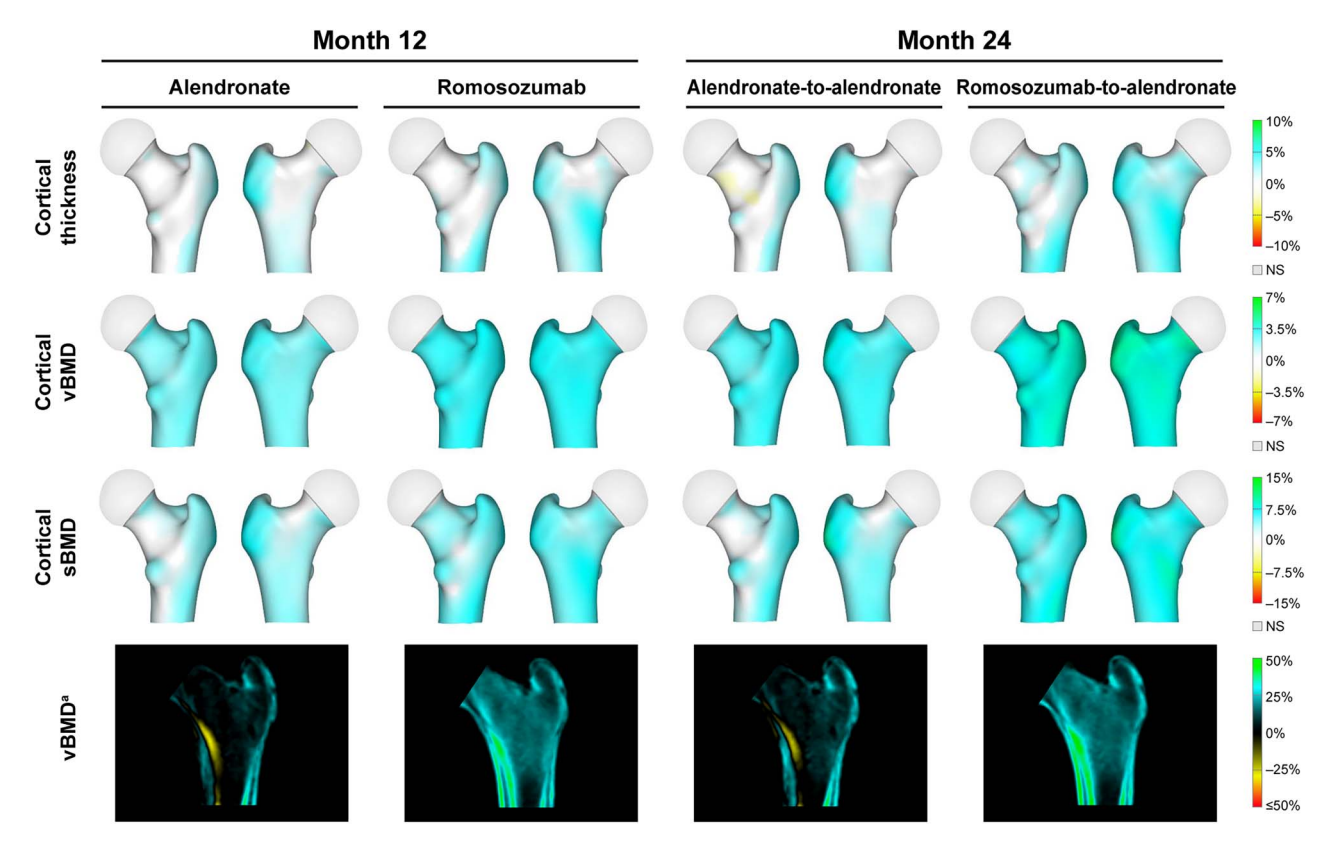


**Figure 6.** Percentage change from baseline to month 12 and month 24 in cortical thickness, cortical vBMD, cortical sBMD, and vBMD for cortical and trabecular compartments by 3D-SHAPER analysis of hip DXA scans in ARCH. Increases in bone parameters are presented in blue–green color; decreases are presented in yellow–red color. Illustrations for each pair of representative femurs per treatment group show the posterior anterior perspective on the left and the anterior posterior perspective on the right. <sup>a</sup>vBMD images include cortical and trabecular compartments; images and data are from a mid-coronal slice. NS = not significant against baseline, Student's *t*-test;

region of interest. Local changes in bone parameters derived with DXA-based 3D SHAPER as presented in Figures 5–7 and Supplementary Figures S2 and S3 should be interpreted with caution. Further studies should be performed to compare 3D representations of average changes calculated using DXA-based 3D-SHAPER with those calculated using QCT.

A recent study by Dudle et al. <sup>37</sup> reported larger systematic differences between bone volume and density estimated by DXA-based 3D-SHAPER and QCT, compared with results reported in another study.<sup>21</sup> The marked systematic differences in bone volume, calculated using the periosteal surface, might be explained by the technique used in Dudle et al.<sup>37</sup> to segment the QCT images, which did not correct for partial volume effects. As shown in a previous study by Treece et al., <sup>38</sup> straightforward segmentation methods tend to overestimate the cortical thickness and therefore, overestimate the bone volume. The segmentation methods used in a previous evaluation study<sup>21</sup> to analyze both DXA-based 3D-SHAPER and QCT data included correction methods for partial volume effects, and were shown to provide accurate estimates of cortical thickness and density, compared with micro-CT data.<sup>22</sup> As mentioned in the study,<sup>21</sup> the systematic differences between DXA-based 3D-SHAPER and QCT vBMD reported might be explained by: (1) the use of ex vivo scans and water bags to account for soft tissues, which can have a significant impact on DXA measurements, 37 and (2) the use of a solid OCT phantom, which provides density measurements 10 to 15% higher, compared with liquid phantoms.<sup>39</sup> The DXAbased 3D-SHAPER software provides density measurements calibrated using a liquid phantom. Further investigation is needed to compare the effect of using liquid vs solid phantoms, and ex vivo vs in vivo data, in studies comparing DXA-based 3D-SHAPER and QCT. The DXA scanner model, acquisition parameters, and calibration are also factors that affect DXA measurements and consequently, DXA-based 3D-SHAPER measurements.<sup>21</sup>

DXA-based 3D-SHAPER analysis may be utilized as a research tool for measuring physiological changes in bone morphology and has the potential to provide a no. of applications and benefits in clinical practice. Within the clinical setting, DXA scans of patients are readily available and could easily be assessed by DXA-based 3D-SHAPER analysis without subjecting patients to additional testing procedures. The technique requires further evaluation of clinical utility in individual patients. By comparison, QCT is not widely available in clinical practice, and where available, obtaining patient QCT scans would require additional testing procedures for patients and exposure to excessive radiation. DXA-based 3D-SHAPER analysis could thus be a convenient methodology to acquire additional compartmental information in patients. Additionally, DXA-based 3D-SHAPER analysis can be performed retrospectively from archived DXA data in studies where QCT was not performed.<sup>23-25</sup> Finally, DXAbased 3D-SHAPER analysis could be used to visually monitor the effect of osteoporosis treatments on both cortical and trabecular bone compartments.

In conclusion, 3D-SHAPER analysis provides a novel technique for estimating changes in cortical and trabecular bone

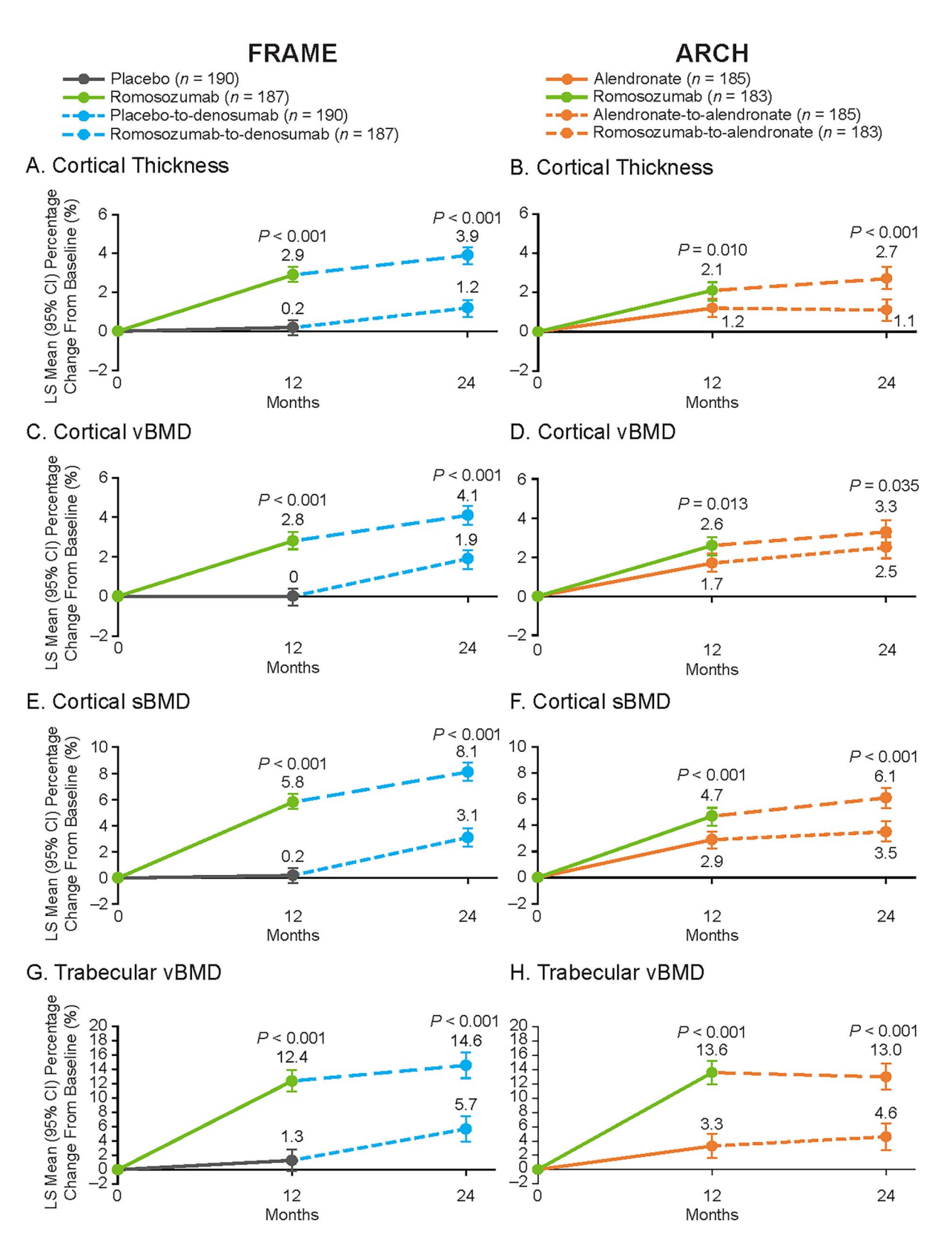


**Figure 7.** Percentage change from baseline to month 12 and month 24 in cortical thickness, cortical vBMD, cortical sBMD, and trabecular vBMD by 3D-SHAPER analysis of hip DXA scans in FRAME (A, C, E, and G) and ARCH (B, D, F, and H). n = no. of women who had completed the 24-mo study period, had provided consent for future research, had TH DXA scans at baseline, month 12, and month 24, and completed the 3D-SHAPER analysis. Treatment group comparisons for percentage change from baseline for bone parameters were assessed by a repeated-measures model adjusting for treatment, visit, treatment-by-visit interaction, baseline value, machine type, and baseline value-by-machine type interaction in FRAME and adjusting for treatment, presence of severe vertebral fracture at baseline, visit, treatment-by-visit interaction, baseline value, machine type and baseline value-by-machine type interaction in ARCH. P values are for the comparison of the 2 treatment groups in each study.

parameters from standard DXA images and also for visualizing the changes in those parameters to monitor treatment effect. Results from 3D-SHAPER analysis of standard hip DXA scans in FRAME and ARCH complement the extensive evidence demonstrating that treatment with romosozumab results in substantial gains in hip cortical and trabecular bone compartments within 1 yr, and that transition to an antiresorptive agent can maintain or augment those gains, thereby contributing to the antifracture efficacy of the drug.

### **Acknowledgments**

Representatives of Amgen Inc. and UCB Pharma designed the study and funded all costs associated with the development of this manuscript. Lisa Humphries, PhD, of Amgen Inc., and Martha Mutomba (on behalf of Amgen Inc.) provided medical writing support.

### **Author contributions**

All authors participated in the interpretation of the data and in drafting the manuscript or revising it critically for important intellectual content. All authors provided final approval for submission of the manuscript for publication. E. Michael Lewiecki (Investigation, Supervision, Writing-Original Draft, and Writing-Reviewing and Editing), Donald Betah (Conceptualization, Methodology, Supervision, Writing-Original Draft, and Writing-Reviewing and Editing), Ludovic Humbert (Conceptualization, Methodology, Formal Analysis, Data Curation, Visualization, and Writing—Reviewing and Editing) Cesar Libanati (Conceptualization, Methodology, and Writing-Reviewing and Editing), Mary Oates (Conceptualization, Methodology, and Writing-Reviewing and Editing), Yifei Shi (Conceptualization, Methodology, Formal Analysis, Data Curation, and Writing-Reviewing and Editing), Renaud Winzenrieth (Conceptualization, Methodology, Formal Analysis, Data Curation, Visualization, and Writing-Reviewing and Editing), Serge Ferrari (Investigation and Writing—Reviewing and Editing), and Fumitoshi Omura (Investigation and Writing-Reviewing and Editing)

### Supplementary material

Supplementary material is available at *Journal of Bone and Mineral Research* online.

### **Funding**

This study was funded by Amgen Inc., UCB Pharma, and Astellas Pharma Inc.

### Conflicts of interest

E.M.L. has received research support and consulting fees from Amgen and Radius Health. M.O. and Y.S. are employees and stockholders of Amgen. D.B. was an employee and is a stockholder of Amgen. L.H. is an employee and stockholder of 3D-SHAPER Medical. R.W. was an employee of 3D-SHAPER Medical. C.L. was an employee and is a stockholder of UCB Pharma. S.F. has received grant/research support from Amgen, UCB Pharma, Agnovos, Alexion, and Labatec and received consulting fees from Amgen, UCB Pharma, Agnovos, Flowbone, Fresenius, Galapagos, and Radius Health. F.O. has nothing to disclose.

### **Data availability**

Qualified researchers may request data from Amgen clinical studies. Complete details are available at the following: http://www.amgen.com/datasharing

#### References

- 1. Morgan EF, Unnikrisnan GU, Hussein AI. Bone mechanical properties in healthy and diseased states. *Annu Rev Biomed Eng.* 2018;20(1):119–143. https://doi.org/10.1146/annurev-bioeng-062117-121139.
- Bouxsein ML, Seeman E. Quantifying the material and structural determinants of bone strength. Best Pract Res Clin Rheumatol. 2009;23(6):741–753. https://doi.org/10.1016/j.berh.2009.09.008.
- 3. Warriner AH, Patkar NM, Curtis JR, et al. Which fractures are most attributable to osteoporosis? *J Clin Epidemiol*. 2011;64(1): 46–53. https://doi.org/10.1016/j.jclinepi.2010.07.007.
- 4. Johnell O, Kanis JA. An estimate of the worldwide prevalence and disability associated with osteoporotic fractures. *Osteoporos Int.* 2006;17(12):1726–1733. https://doi.org/10.1007/s00198-006-0172-4.
- Hansen D, Pelizzari P, Pyenson B. Medicare Cost of Osteoporotic Fractures –2021 Updated Report: The Clinical and Cost Burden of Fractures Associated with Osteoporosis. Commissioned by the Bone Health and Osteoporosis Foundation. https://www.millima n.com/en/insight/-/media/milliman/pdfs/2021-articles/3-30-21-Medicare-Cost-Osteoporotic-Fractures.ashx; 2021: Accessed November 22, 2023.
- Austin M, Yang Y-C, Vittinghoff E, et al. Relationship between bone mineral density changes with denosumab treatment and risk reduction for vertebral and nonvertebral fractures. *J Bone Miner Res.* 2012;27(3):687–693. https://doi.org/10.1002/jbmr.1472.
- Cosman F, Crittenden DB, Ferrari S, et al. FRAME study: the foundation effect of building bone with 1 year of romosozumab leads to continued lower fracture risk after transition to denosumab. *J Bone Miner Res.* 2018;33(7):1219–1226. https://doi.org/10.1002/jbmr.3427.
- 8. Ferrari S, Adachi JD, Lippuner K, et al. Further reductions in nonvertebral fracture rate with long-term denosumab treatment in the FREEDOM open-label extension and influence of hip bone mineral density after 3 years. *Osteoporos Int*. 2015;26(12): 2763–2771. https://doi.org/10.1007/s00198-015-3179-x.
- 9. Kendler DL, Marin F, Zerbini CAF, et al. Effects of teriparatide and risedronate on new fractures in post-menopausal women with severe osteoporosis (VERO): a multicentre, double-blind, double-dummy, randomised controlled trial. *Lancet*. 2018;391(10117): 230–240. https://doi.org/10.1016/S0140-6736(17)32137-2.
- Saag KG, Zanchetta JR, Devogelaer J-P, et al. Effects of teriparatide versus alendronate for treating glucocorticoid-induced osteoporosis: thirty-six-month results of a randomized, doubleblind, controlled trial. *Arthritis Rheum*. 2009;60(11):3346–3355. https://doi.org/10.1002/art.24879.
- 11. Langdahl BL, Libanati C, Crittenden DB, et al. Romosozumab (sclerostin monoclonal antibody) versus teriparatide in postmenopausal women with osteoporosis transitioning from oral bisphosphonate therapy: a randomised, open-label, phase 3 trial. *Lancet*. 2017;390(10102):1585–1594. https://doi.org/10.1016/S0140-6736(17)31613-6.
- Cosman F, Miller PD, Williams GC, et al. Eighteen months
  of treatment with subcutaneous abaloparatide followed by 6
  months of treatment with alendronate in postmenopausal women
  with osteoporosis: results of the ACTIVExtend trial. *Mayo*Clin Proc. 2017;92(2):200–210. https://doi.org/10.1016/j.mayo
  cp.2016.10.009.
- 13. Bouxsein ML, Eastell R, Lui L-Y, et al. Change in bone density and reduction in fracture risk: a meta-regression of published trials. *J Bone Miner Res.* 2019;34(4):632–642. https://doi.org/10.1002/jbmr.3641.
- 14. Keaveny TM, McClung MR, Genant HK, et al. Femoral and vertebral strength improvements in postmenopausal women with osteoporosis treated with denosumab. *J Bone Miner Res.* 2014;29(1): 158–165. https://doi.org/10.1002/jbmr.2024.
- Bauer JS, Kohlmann S, Eckstein F, Mueller D, Lochmüller EM, Link TM. Structural analysis of trabecular bone of the proximal femur using multislice computed tomography: a comparison

- with dual x-ray absorptiometry for predicting biomechanical strength in vitro. *Calcif Tissue Int.* 2006;78(2):78–89. https://doi.org/10.1007/s00223-005-0070-3.
- Nawathe S, Akhlaghpour H, Bouxsein ML, Keaveny TM. Microstructural failure mechanisms in the human proximal femur for sideways fall loading. *J Bone Miner Res.* 2014;29(2):507–515. https://doi.org/10.1002/jbmr.2033.
- 17. Fields AJ, Lee GL, Liu XS, Jekir MG, Guo XE, Keaveny TM. Influence of vertical trabeculae on the compressive strength of the human vertebra. *J Bone Miner Res.* 2011;26(2):263–269. https://doi.org/10.1002/jbmr.207.
- Ammann P, Rizzoli R. Bone strength and its determinants. Osteoporos Int. 2003;14(S3):13–S18. https://doi.org/10.1007/s00198-002-1345-4.
- Osterhoff G, Morgan EF, Shefelbine SJ, Karim L, McNamara LM, Augat P. Bone mechanical properties and changes with osteoporosis. *Injury*. 2016;47(Suppl 2):S11–S20. https://doi.org/10.1016/ S0020-1383(16)47003-8.
- Keaveny TM. Biomechanical computed tomography—noninvasive bone strength analysis using clinical computed tomography scans. *Ann N Y Acad Sci.* 2010;1192(1):57–65. https://doi.org/10.1111/j.1749-6632.2009.05348.x.
- Humbert L, Martelli Y, Fonolla R, et al. 3D-DXA: assessing the femoral shape, the trabecular macrostructure and the cortex in 3D from DXA images. *IEEE Trans Med Imaging*. 2017;36(1):27–39. https://doi.org/10.1109/TMI.2016.2593346.
- Humbert L, Hazrati Marangalou J, Del Río Barquero LM, van Lenthe GH, van Rietbergen B. Technical note: cortical thickness and density estimation from clinical CT using a prior thicknessdensity relationship. *Med Phys.* 2016;43(4):1945–1954. https:// doi.org/10.1118/1.4944501.
- Winzenrieth R, Ominsky MS, Wang Y, Humbert L, Weiss RJ. Differential effects of abaloparatide and teriparatide on hip cortical volumetric BMD by DXA-based 3D modeling. Osteoporos Int. 2021;32(3):575–583. https://doi.org/10.1007/s00198-020-05806-1.
- Winzenrieth R, Humbert L, Boxberger JI, Weiss RJ, Wang Y, Kostenuik P. Abaloparatide effects on cortical volumetric BMD and estimated strength indices of hip subregions by 3D-DXA in women with postmenopausal osteoporosis. *J Clin Densitom*. 2022;25(3):392–400. https://doi.org/10.1016/j.jocd.2021.11.007.
- 25. Winzenrieth R, Kostenuik P, Boxberger J, Wang Y, Humbert L. Proximal femur responses to sequential therapy with abaloparatide followed by alendronate in postmenopausal women with osteoporosis by 3D modeling of hip dual-energy x-ray absorptiometry (DXA). *JBMR Plus*. 2022;6(4):e10612. https://doi.org/10.1002/jbm4.10612.
- Humbert L, Bagué A, Di Gregorio S, et al. DXA-based 3D analysis of the cortical and trabecular bone of hip fracture postmenopausal women: a case-control study. *J Clin Densitom*. 2020;23(3):403–410. https://doi.org/10.1016/j.jocd.2018. 11.004.
- McClung MR, Grauer A, Boonen S, et al. Romosozumab in postmenopausal women with low bone mineral density. N Engl J Med. 2014;370(5):412–420. https://doi.org/10.1056/NEJMoa130 5224.

- 28. Padhi D, Jang G, Stouch B, Fang L, Posvar E. Single-dose, placebocontrolled, randomized study of AMG 785, a sclerostin monoclonal antibody. *J Bone Miner Res.* 2011;26(1):19–26. https://doi.org/10.1002/jbmr.173.
- 29. McClung MR, Brown JP, Diez-Perez A, et al. Effects of 24 months of treatment with romosozumab followed by 12 months of denosumab or placebo in postmenopausal women with low bone mineral density: a randomized, double-blind, phase 2, parallel group study. *J Bone Miner Res.* 2018;33(8):1397–1406. https://doi.org/10.1002/jbmr.3452.
- 30. Cosman F, Crittenden DB, Adachi JD, et al. Romosozumab treatment in postmenopausal women with osteoporosis. *N Engl J Med.* 2016;375(16):1532–1543. https://doi.org/10.1056/NEJMoa1607948.
- Saag KG, Petersen J, Brandi ML, et al. Romosozumab or alendronate for fracture prevention in women with osteoporosis. N Engl J Med. 2017;377(15):1417–1427. https://doi.org/10.1056/NEJMoa1708322.
- 32. Brown JP, Engelke K, Keaveny TM, et al. Romosozumab improves lumbar spine bone mass and bone strength parameters relative to alendronate in postmenopausal women: results from the Active-Cntrolled Fracture Study in Postmenopausal Women with Osteoporosis at High Risk (ARCH) trial. *J Bone Miner Res.* 2021;36(11): 2139–2152. https://doi.org/10.1002/jbmr.4409.
- 33. Chavassieux P, Chapurlat R, Portero-Muzy N, et al. Bone-forming and antiresorptive effects of romosozumab in postmenopausal women with osteoporosis: bone histomorphometry and microcomputed tomography analysis after 2 and 12 months of treatment. *J Bone Miner Res.* 2019;34(9):1597–1608. https://doi.org/10.1002/jbmr.3735.
- 34. Genant HK, Engelke K, Bolognese MA, et al. Effects of romosozumab compared with teriparatide on bone density and mass at the spine and hip in postmenopausal women with low bone mass. *J Bone Miner Res.* 2017;32(1):181–187. https://doi.org/10.1002/jbmr.2932.
- 35. Poole KE, Treece GM, Pearson RA, et al. Romosozumab enhances vertebral bone structure in women with low bone density. *J Bone Miner Res.* 2022;37(2):256–264. https://doi.org/10.1002/jbmr.4465.
- 36. Keaveny TM, Crittenden DB, Bolognese MA, et al. Greater gains in spine and hip strength for romosozumab compared with teriparatide in postmenopausal women with low bone mass. *J Bone Miner Res.* 2017;32(9):1956–1962. https://doi.org/10.1002/jbmr.3176.
- Dudle A, Gugler Y, Pretterklieber M, Ferrari S, Lippuner K, Zysset P. 2D-3D reconstruction of the proximal femur from DXA scans: evaluation of the 3D-Shaper software. Front Bioeng Biotechnol. 2023;11:111020. https://doi.org/10.3389/fbioe.2023.1111020
- Treece GM, Gee AH, Mayhew PM, Poole KE. High resolution cortical bone thickness measurement from clinical CT data. *Med Image Anal.* 2010;14(3):276–290. https://doi.org/10.1016/j.media.2010.01.003.
- Faulkner KG, Glüer CC, Grampp S, Genant HK. Cross-calibration of liquid and solid QCT calibration standards: corrections to the UCSF normative data. Osteoporos Int. 1993;3(1):36–42. https:// doi.org/10.1007/BF01623175.